



ISSN
2217-5369
(print version ceased in 2023)
2217-5660 (online)

www.foodandfeed.fins.uns.ac.rs

FOOD AND FEED RESEARCH

Journal of the Institute of Food Technology – FINS
University of Novi Sad



UDK 577.112:544.77:66.021.4

<https://doi.org/10.5937/ffr0-61995>

Short communication

STRUCTURAL CHARACTERIZATION AND STORAGE STABILITY OF HEAT-INDUCED LACTOFERRIN-SODIUM CASEINATE COMPLEXES AT DIFFERENT MASS RATIOS

Yaping Sun*, Zhengtao Zhao

Jining Cisen Pharmaceutical Co. Ltd, 272073, Jining, Shandong, China

Abstract: Sodium caseinate (NaCas) forms complexes with lactoferrin (LF), yet the structural characteristics and stability of these complexes before and after heating are not well understood. This study demonstrated that lactoferrin and sodium caseinate exhibit weak electrostatic interactions prior to heating. Upon heating at 90 °C for 10 minutes, these interactions were significantly enhanced, resulting in the formation of stable lactoferrin/sodium caseinate complexes at ratios of 2:1 and 1:1. Complexes formed at a 1:2 ratio initially exhibited smaller particle sizes and lower turbidity but subsequently precipitated during storage. Conversely, complexes at 2:1 and 1:1 ratios maintained consistent turbidity and particle size over 20 days, indicating excellent long-term stability. These findings reveal the important role of NaCas in stabilizing LF during heat treatment and storage, providing valuable insights for the development of stable protein-based functional food ingredients.

Key words: *colloidal stability, heat treatment, turbidity, particle size, cation exchange chromatography, zeta potential*

INTRODUCTION

Lactoferrin (LF) is an iron-binding glycoprotein that exists in different forms depending on its iron saturation level: holo-LF (>90% iron saturation), native-LF (15-20%), and apo-LF (iron-depleted) (Ward, Paz & Conneely, 2005; Bokkhim, Bansal, Grondahl & Bhandari, 2010).

LF exhibits anti-inflammatory, antiviral, and enzymatic activities, which are closely linked to its thermal stability (Sreedhara et al., 2010). Among those forms, holo-LF shows high heat stability ($T_m \approx 90$ °C at neutral pH), while native- and apo-LF denature at temperatures above 70 °C, causing aggregation and loss of

functionality (Sreedhara et al., 2010; Stănciuc et al., 2013). To mitigate thermal denaturation, various strategies have been used to preserve LF structure during thermal processing, such as the addition of anionic polysaccharides (Li, Lan & Zhao, 2019; Xu, Zhao, Guo & Du, 2019) and proteins (Li & Zhao, 2017; Zhao, Lan, Li & Wang, 2018).

Sodium Caseinate (NaCas), the sodium salt of caseins, possesses a random coil structure, an isoelectric point of approximately 4.6, and excellent heat stability (Wang & Zhao, 2022). LF and NaCas are known to interact mainly

through electrostatic forces, improving emulsion stability (HadjSadok et al., 2008). However, previous studies have found that LF-NaCas interactions are relatively weak before heating, likely due to ionic screening (Anema, 2021; De Kruif, Pedersen, Huppertz & Anema, 2013).

Previous work demonstrated that thermal treatment significantly enhances LF-NaCas interactions through electrostatic, hydrophobic, and disulfide bonds (Li & Zhao, 2017). Nevertheless, the detailed structural characteristics of these complexes and their stability during storage remain insufficiently understood.

Heat-induced complexation has also been reported in LF systems with whey proteins (Li & Zhao, 2018; Anema, 2021) and anionic polysaccharides (Li et al., 2019; Jiang et al., 2024), where thermal unfolding enhances electrostatic attraction and promotes hydrophobic interactions and disulfide bond formation, resulting in more stable complexes.

Despite these advances, the specific role of sodium caseinate in such systems-particularly in relation to long-term colloidal stability-has not been thoroughly investigated. Therefore, the objective of this study was to characterize the structural properties and storage stability of LF-NaCas complexes formed at different mass ratios.

Dynamic light scattering and cation exchange chromatography were used to analyze structural features, while turbidity, particle size, and visual appearance were monitored to evaluate storage stability.

MATERIALS AND METHODS

Materials

LF (>90%, batch# LF201705, Fonterra, New Zealand) and NaCas (batch# C8654, Sigma-Aldrich, USA) solutions (10 g kg⁻¹) were prepared in distilled water, hydrated overnight, filtered (0.45 μm), and adjusted to pH 7.0 using either 1 mol L⁻¹ NaOH or HCl as needed.

Mixtures with LF:NaCas ratios at 2:1, 1:1, and 1:2 (total protein 10 g kg⁻¹) were stirred for 1 h at 22 °C, heated (90 °C, 10 min), cooled, and stored at 22 °C. The stability and physicochemical properties of the samples were monitored at various storage intervals: 1, 5, 10, 15, and 20 days.

AKTA chromatography

Separation of LF and NaCas was performed using cation exchange chromatography on an AKTA purifier system (900 series, GE Biosciences, Baied-Urfe, Quebec, Canada), equipped with a UV-900 detector set at 280 nm. Prior to injection, all samples were filtered through 0.45 μm membrane filters (Millipore

Corporation, Bedford, MA). A 500 μL aliquot of each sample was injected onto a Hitrap™ SP HP column (1 mL), packed with cross-linked agarose functionalized with sulfonate groups (SO₃⁻) on the surface.

The mobile phase A consisted of 50 mmol L⁻¹ phosphate buffer at pH 7.7, whereas mobile phase B contained the same phosphate buffer supplemented with 2 mol L⁻¹ NaCl at pH 7.7. A linear gradient elution was carried out over a total runtime of 30 minutes at a flow rate of 1 mL min⁻¹.

SDS-PAGE

Sodium dodecyl sulfate-polyacrylamide gel electrophoresis (SDS-PAGE) was performed according to the method described by Zhao and Corredig (2016). Briefly, eluents were diluted 1:1 with sample buffer containing 0.5 mol L⁻¹ Tris-HCl (pH 6.8), 20 g kg⁻¹ SDS, 190 g kg⁻¹ glycerol, 0.5 g kg⁻¹ 2-mercaptoethanol, and 0.1 g kg⁻¹ bromophenol blue.

The samples were then heated at 95 °C for 5 minutes, followed by equilibration at room temperature for 20 minutes. Subsequently, 10 μL aliquots of the prepared samples were loaded onto polyacrylamide gels composed of 150 g kg⁻¹ resolving gel and 40 g kg⁻¹ stacking gel.

Electrophoresis was conducted at 200 V for 45 minutes using a Bio-Rad Power Pac HC electrophoresis unit (Hercules, CA). The gels were stained with Coomassie Brilliant Blue using a 5:1:4 mixture of methanol, acetic acid, and Milli-Q water for 30 minutes, then destained twice for 1 hour each in a 4.5:1:4.5 mixture of methanol, acetic acid, and Milli-Q water.

Turbidity

Turbidity (A₆₀₀), defined as the absorbance at 600 nm, was measured at 22 °C using a Hitachi UV-1100 (Hitachi High-Technologies Corporation, Tokyo, Japan) with 2 mL samples in 10 mm cuvettes.

Zeta potential

Zeta potential was determined by laser Doppler electrophoresis (Nano-S Zetasizer, DTS1060 cell) using a Malvern Nano-S (ZEN3600, Malvern Panalytical Ltd, Malvern, UK) equipped with a DTS1060 capillary cell. Results were expressed as absolute values in millivolts (mV).

Particle size

Particle size was measured by dynamic light scattering (DLS) (Zetasizer Nano, 173° backscatter) on undiluted samples; results are intensity-weighted diameters from cumulants analysis, with distributions plotted by volume.

Data analysis

Measurements were done in triplicate; results are mean \pm standard deviation (SD). Significance was tested by ANOVA with Tukey's HSD ($p < 0.05$, Minitab v. 15).

RESULTS AND DISCUSSION

Fig. 1 presents the average hydrodynamic diameters of the various samples. Before heating, addition of NaCas at the LF/NaCas ratio of 2:1 reduced particle size from 80 ± 3 nm to 37 ± 1 nm, indicating the formation of LF-NaCas complexes. Increasing NaCas contents to ratios of 1:1 and 1:2 resulted in larger diameters of 59 ± 11 nm and 126 ± 3 nm, likely due to the larger native size of NaCas (203 ± 3 nm). After heating, LF alone precipitated due to denaturation and aggregation. At the ratio of 2:1, the com-

plex size increased to 194 ± 9 nm without visible precipitation. In contrast, the particle sizes at the 1:1 and 1:2 ratios decreased to approximately 62 ± 1 nm, suggesting improved thermal stability. These findings indicate that a higher NaCas level ($\geq 1:1$) effectively mitigates LF denaturation and aggregation upon heating, consistent with previous zeta potentials shift from positive to negative upon mixing (Li & Zhao, 2017).

Fig. 2A illustrates the elution profiles of LF and NaCas prior to thermal treatment. Before heating, NaCas and LF were eluted at 0-5 minutes and 10-16 minutes, respectively, with peak areas correlating linearly with concentration (Fig. 2C), suggesting weak interaction under native conditions due to sodium screening (Li & Zhao, 2018).

After heating (Fig. 2B), the LF peak area in the control (LF only) decreased markedly due to the formation of large aggregates during heating, which was subsequently removed during the filtration step. At the LF/NaCas ratio of 2:1, the LF peak area increased by 46% following heating. In comparison, no significant changes were observed in the 1:1 and 1:2 samples.

The observed increase in peak area at the 2:1 ratio may be attributed to two potential mechanisms: (1) NaCas associating with LF molecules during heat-induced complexation, or (2) thermal denaturation of LF exposing previously buried aromatic residues, enhancing UV absorbance (Li et al., 2019).

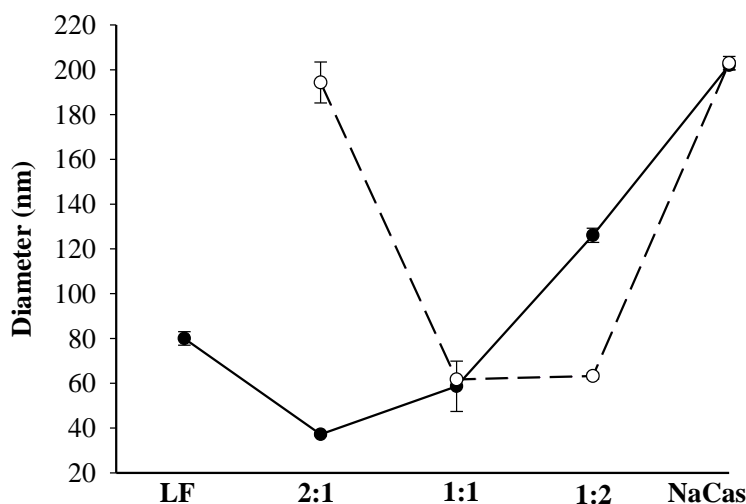


Figure 1. Hydrodynamic radius for samples before (filled circles) and after (empty circles) heating at different LF/NaCas ratios.

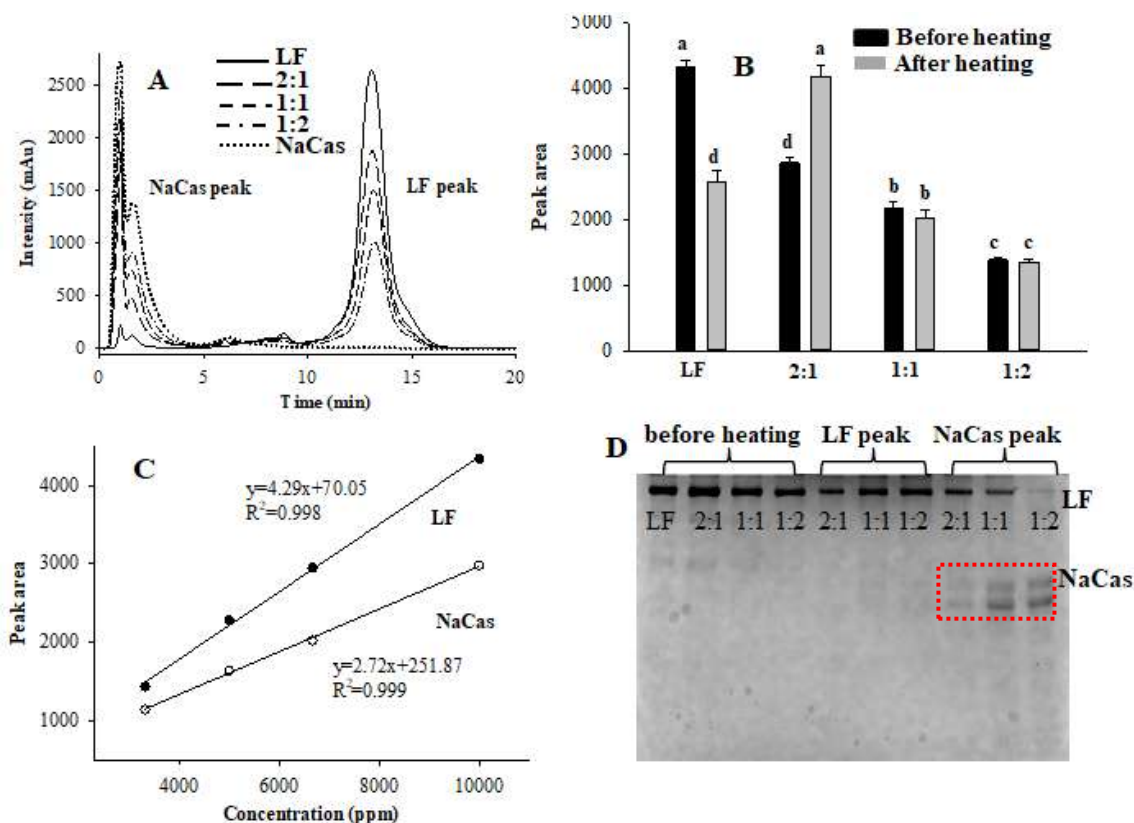


Figure 2. LF elution profiles (A), LF peak areas (B), linear relationship (C) between peak areas and protein concentration for LF (filled circles) and NaCas (empty circles), and SDS-PAGE electrophoresis (D) of elutes from SEC peaks for different samples before (lane 1-4) and after (lane 5-10) heating.

To investigate these possibilities, SDS-PAGE was used to analyze the protein composition of the eluted fractions (Fig. 2D). Lanes 1-4 (before heating) showed strong LF bands but no detectable NaCas bands, confirming minimal interaction under non-heated conditions (Li & Zhao, 2017). After heating (lanes 5-7), LF band intensity decreased markedly in all samples, most notably at the 2:1 ratio, supporting the hypothesis that thermal denaturation and aggregation contributed to the increased peak area in the chromatogram, rather than NaCas attachment alone. SDS-PAGE analysis of the NaCas peaks post-heating (lanes 8-10) revealed that increasing NaCas band intensity with higher NaCas content and clear LF bands, indicating that a portion of LF was co-eluted with NaCas due to complex formation. LF band intensity declined with decreasing LF/NaCas ratios, suggesting more LF incorporation into NaCas aggregates when NaCas was in excess. Overall, these results imply that during heating, LF was encapsulated or embedded within NaCas aggregates rather than simply adhering to their sur-

face, providing both electrostatic shielding and steric stabilization to enhance complex solubility and stability (Li & Zhao, 2017).

Figure 3A shows optical images of heated LF/NaCas mixtures on day 1 and day 20 of storage. It is important to note that the influence of protein hydrolysis by plasmin can be considered negligible in this study, as plasmin activity is effectively inhibited by heating at 90 °C for durations exceeding 30 seconds (Gazi, Vilalva & Huppertz, 2014). After heating, LF alone precipitated, indicating severe aggregation. In contrast, the heated NaCas solution exhibited stable turbidity and particle size for up to 20 days. For the mixtures, the sample with a 2:1 ratio appeared white and turbid, consistent with LF denaturation and aggregation (Betz, 1993; Li & Zhao, 2017). The 1:1 and 1:2 samples were initially transparent but behaved differently during storage. The 1:1 mixture remained clear throughout the 20-day storage, whereas 1:2 sample developed turbidity by day 5 and showed visible precipitates thereafter, as shown in Fig. 3A.

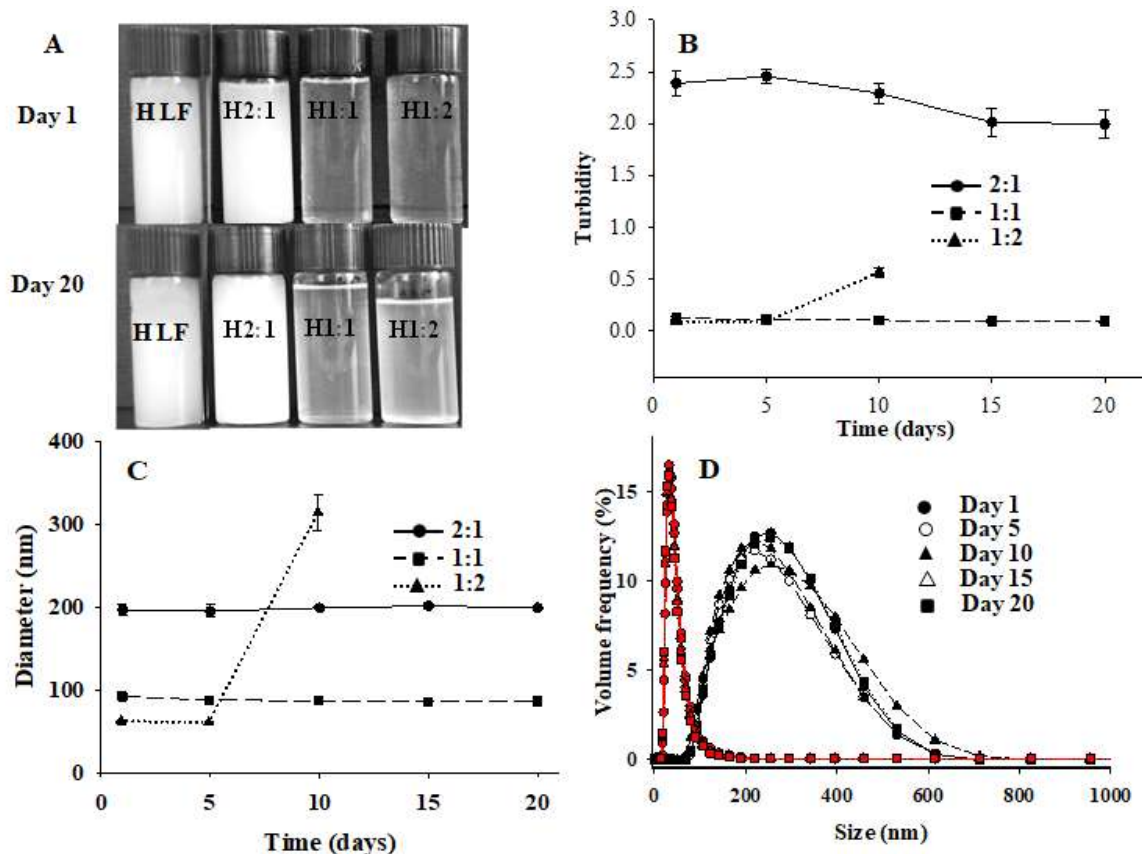


Figure 3. Optical images (A) for samples at different LF/NaCas ratios after heat treatment at day 1 (top) and day 20 (bottom), changes of turbidity (B), Z-diameter (C) for heat-induced LF/NaCas complexes during storage, and size distribution of heated LF/NaCas complexes with ratio of 2:1 (black) and 1:1 (red) at different storage days

The temporal evolution of turbidity during storage is quantitatively summarized in Fig. 3B. The sample with a 2:1 ratio showed the highest turbidity (~2.2), consistent with its visibly turbid appearance. In contrast, the 1:1 and 1:2 samples had low initial turbidity (~0.1) after heating. No significant turbidity changes occurred over time for the 2:1 and 1:1 samples, indicating stable LF/NaCas complexes. Conversely, the 1:2 sample exhibited a marked turbidity increase after 5 days, which further intensified by day 10, consistent with precipitation observed visually.

A plausible explanation for this instability at the 1:2 ratio is the presence of excess free NaCas molecules leading to depletion flocculation (Jenkins & Snowden, 1996). In this scenario, free NaCas molecules, which are negatively charged, repel the similarly charged LF/NaCas complexes. This electrostatic repulsion prevents close approach between complexes, resulting in a higher concentration of free NaCas in the bulk solution and a lower concentration in the interstitial spaces. Consequently, an osmotic pres-

sure gradient arises, driving water from the inter-complex regions into the bulk solution. This dehydration promotes aggregation and eventual precipitation.

Fig. 3C shows changes in hydrodynamic diameter during storage. The 2:1 sample exhibited a large, stable diameter of approximately 204 nm, while the 1:1 sample maintained a smaller, stable diameter of approximately 61 nm. In contrast, the 1:2 sample increased sharply to 314 nm by day 5, consistent with increased turbidity and precipitation.

Fig. 3D compares size distributions of 2:1 (black peaks) and 1:1 (red peaks) samples. Both showed stable unimodal distributions for over 20 days, with the 1:1 sample having a narrower distribution. LF-NaCas interaction disassembled and reorganized large NaCas aggregates into smaller particles (see Fig. 1). Upon mixing, NaCas dissociated and coated LF molecules, as shown by the zeta potential shift from positive to negative (Li & Zhao, 2017). This charged hydrated casein layer provided electrostatic and steric repulsions, preventing aggregation. The

constant size distribution confirms that LF-NaCas complexation is stabilized by hydro-phobic interactions and disulfide bonds, ensuring long-term colloidal stability at both protein ratios.

CONCLUSIONS

The interaction between LF and NaCas before heat treatment is limited and mainly driven by electrostatic attraction. This interaction weakens under low ionic strength, as shown by cation exchange chromatography profiles. Heat treatment significantly enhances LF-NaCas interactions, leading to the formation of stable complexes that inhibit LF denaturation and aggregation. The structure and stability of these complexes strongly depend on the LF-to-NaCas ratio. Complexes at a 2:1 ratio display larger particle sizes and higher turbidity than those at 1:1 or 1:2 ratios. Excess free NaCas in the bulk phase negatively impacts storage stability, likely due to depletion flocculation.

Overall, this study highlights NaCas as a promising functional ingredient to improve the heat stability of LF-enriched products, especially functional beverages. Nonetheless, further studies are needed to explore complex stability under varying pH and ionic strength, to evaluate their potential in stabilizing oil-in-water emulsions, and to validate their performance in real food matrices (e.g., fortified beverages, dairy products) for broader industrial applications.

AUTHOR CONTRIBUTIONS

Conceptualization, methodology, investigation, formal analysis, validation, writing-original draft preparation, writing-review and editing, Y.S.; Supervision, revising, Z.Z.

DATA AVAILABILITY STATEMENT

Data contained within the article.

ACKNOWLEDGEMENTS

The authors would like to express their gratitude to all colleagues and institutions that contributed to this research through their valuable support and collaboration.

CONFLICT OF INTEREST

The authors declare no conflict of interest. The funders had no role in the design of the study; in the collection, analyses, or interpretation of

data; in the writing of the manuscript, or in the decision to publish the results.

REFERENCES

- Anema, S. G. (2021). Spontaneous interaction between whey protein isolate proteins and lactoferrin: Effect of heat denaturation. *International Dairy Journal*, *113*, 104887. <https://doi.org/10.1016/j.idairyj.2020.104887>
- Betz, S. F. (1993). Disulfide bonds and the stability of globular proteins. *Protein Science*, *2*, 1551-1558. doi: 10.1002/pro.5560021002.
- Bokkhim, H., Bansal, N., Grondahl, L., & Bhandari, B. (2010). Physico-chemical properties of different forms of bovine lactoferrin. *Food Chemistry*, *141*, 3007-3013. <https://doi.org/10.1016/j.foodchem.2013.05.139>.
- De Kruif, C. G., Pedersen, J., Huppertz, T., & Anema, S. G. (2013). Coacervates of lactotransferrin and β - or κ -casein: structure determined using SAXS. *Langmuir* *29*, 10483-10490. <https://doi.org/10.1021/la402236f>.
- Gazi, I., Vilalva, I., & Huppertz, T. (2014). Plasmin activity and proteolysis in milk protein ingredients. *International Dairy Journal*, *38*, 208-212. <https://doi.org/10.1016/j.idairyj.2013.11.012>.
- Jenkins, P., & Snowden, M. (1996). Depletion flocculation in colloidal dispersions. *Advances in Colloid and Interface Science*, *68*, 57-96. [https://doi.org/10.1016/S0001-8686\(96\)90046-9](https://doi.org/10.1016/S0001-8686(96)90046-9).
- Jiang, H., Zhang, T., Pan, Y., Yang, H., Xu, X., Han, J., & Liu, W. (2024). Thermal stability and in vitro biological fate of lactoferrin-polysaccharide complexes. *Food Research International* *182*, 114182. <https://doi.org/10.1016/j.foodres.2024.114182>
- Li, Q., & Zhao, Z. (2017). Formation of lactoferrin/sodium caseinate complexes and their adsorption behavior at the air/water interface. *Food Chemistry*, *232*, 697-703. <https://doi.org/10.1016/j.foodchem.2017.04.072>
- Li, Q., & Zhao, Z. (2018). Interaction between lactoferrin and whey proteins and its influence on the heat-induced gelation of whey proteins. *Food Chemistry*, *252*, 92-98. <https://doi.org/10.1016/j.foodchem.2018.01.114>
- Li, Q., Lan, H., & Zhao, Z. (2019). Protection effect of sodium alginate against heat-induced structural changes of lactoferrin molecules at neutral pH. *LWT-Food Science and Technology*, *99*, 513-518. <https://doi.org/10.1016/j.lwt.2018.10.019>
- Sreedhara, A., Flengsrud, R., Langsrud, T., Kaul, P., Prakash, V., Krowarsch, D., & Vegarud, G. E. (2010). Structural characteristic, pH and thermal stabilities of apo and holo forms of caprine and bovine lactoferrins. *Biometals*, *23*, 1159-1170. DOI: 10.1007/s10534-010-9366-5.
- Stănciuc, N., Aprodu, I., Răpeanu, G., van der Plancken, I., Bahrim, G., Hendrickx, M. (2013). Analysis of the Thermally induced structural changes of bovine lactoferrin. *Journal of Agricultural and Food Chemistry*, *61*, 2234-2243. <https://doi.org/10.1021/jf305178s>.
- Wang, X., & Zhao, Z. (2022). Improved encapsulation capacity of casein micelles with modified structure. *Journal of Food Engineering* *333*, 111138. <https://doi.org/10.1016/j.jfoodeng.2022.111138>.
- Ward, P. P., Paz, E., & Conneely, O. M. (2005). Multifunctional roles of lactoferrin: A critical over-

- view. *Cellular and Molecular Life Sciences*, 62, 2540-2548. <https://doi.org/10.1007/s00018-005-5369-8>
- Xu, K., Zhao, Z., Guo, M., & Du, J. (2019). Conjugation between okra polysaccharide and lactoferrin and its inhibition effect on thermal aggregation of lactoferrin at neutral pH. *LWT-Food Science and Technology*, 107, 125-131. <https://doi.org/10.1016/j.lwt.2019.02.082>
- Zhao, Z., & Corredig, M. (2016). Serum composition of milk subjected to re-equilibration by dialysis at different temperatures, after pH adjustments. *Journal of Dairy Science*, 99, 2588-2593. <https://doi.org/10.3168/jds.2015-9917>
- Zhao, Z., Lan, H., Li, Q., & Wang, L. (2018). Stability of heat-induced lactoferrin-sodium caseinate complexes: effects of pH and ionic strength. *Journal of Food Measurement and Characterization*, 12, 1896-1903. <https://doi.org/10.1007/s11694-018-9803-7>

STRUKTURNA KARAKTERIZACIJA I STABILNOST PRI SKLADIŠTENJU KOMPLEKSA LAKTOFERINA I NATRIJUM-KAZEINATA INDUKOVANIH TOPLOTOM PRI RAZLIČITIM MASENIM ODNOSIMA

Yaping Sun*, Zhengtao Zhao

Jining Cisen Pharmaceutical Co. Ltd, 272073, Đinin, Šendong, Kina

Sažetak: Natrijum-kazeinat formira komplekse sa laktoferinom, ali strukturne karakteristike i stabilnost ovih kompleksa pre i posle zagrevanja nisu dovoljno razjašnjene. Ova studija je pokazala da laktoferin i natrijum-kazeinat ispoljavaju slabe elektrostatičke interakcije pre zagrevanja. Nakon zagrevanja na 90 °C tokom 10 minuta, ove interakcije su značajno pojačane, što je rezultovalo formiranjem stabilnih kompleksa laktoferin/natrijum-kazeinat pri odnosima 2:1 i 1:1, respektivno. Kompleksi formirani u proporciji 1:2 u početku su pokazivali manju veličinu čestica i nižu zamućenost, ali su se naknadno taložili tokom skladištenja. Suprotno tome, kompleksi pri odnosima 2:1 i 1:1 kazeinata prema laktoferinu održali su konzistentnu zamućenost i veličinu čestica tokom 20 dana, što ukazuje na odličnu dugoročnu stabilnost. Ovi nalazi otkrivaju važnu ulogu Na-kazeinata u stabilizaciji laktoferina tokom toplotne obrade i skladištenja, pružajući dragocene uvide za razvoj stabilnih proteinskih funkcionalnih sastojaka hrane.

Ključne reči: koloidna stabilnost, toplotni tretman, zamućenost, veličina čestica, katjon izmenjivačka hromatografija, zeta potencijal

Received: 07 October 2025/ Received in revised form: 20 April 2026 / 24 April 2026/ Accepted: 24 April 2026

Available online: June 2026



This open-access article is licensed under the Creative Commons Attribution 4.0 International License. To view a copy of this license, visit <https://creativecommons.org/licenses/by/4.0/> or send a letter to Creative Commons, PO Box 1866, Mountain View, CA 94042, USA.

© The Author(s) 0000